Annals of Botany **123**: 901–915, 2019
doi: 10.1093/aob/mcy228, available online at www.academic.oup.com/aob

ANNALS OF BOTANY
Founded 1887

Heterochronic reproductive developmental processes between diploid and tetraploid cytotypes of *Paspalum rufum*

Mariano Soliman[1], Francisco Espinoza[2], Juan Pablo A. Ortiz[1] and Luciana Delgado[1,*]

[1]Instituto de Investigaciones en Ciencias Agrarias de Rosario (IICAR), CONICET-UNR/Laboratorio de Biología Molecular, Facultad de Ciencias Agrarias, Universidad Nacional de Rosario. Campo Experimental Villarino, Zavalla, Provincia de Santa Fe, (S2125ZAA), Argentina and [2]Instituto de Botánica del Nordeste (IBONE), CONICET-UNNE, Facultad de Ciencias Agrarias, Universidad Nacional del Nordeste, Casilla de Correo 209, (3400), Corrientes, Argentina
** For correspondence. E-mail luciana.delgado@conicet.gov.ar*

Received: 7 June 2018 Returned for revision: 27 October 2018 Editorial decision: 22 November 2018 Accepted: 28 November 2018
Published electronically 21 December 2018

• **Background and Aims** Apomixis is an asexual reproductive mode via seeds that generate maternal clonal progenies. Although apomixis in grasses is mainly expressed at the polyploid level, some natural diploid genotypes of *Paspalum rufum* produce aposporous embryo sacs in relatively high proportions and are even able to complete apomixis under specific conditions. However, despite the potential for apomixis, sexuality prevails in diploids, and apomixis expression is repressed for an as yet undetermind reason. Apomixis is thought to derive from a deregulation of one or a few components of the sexual pathway that could be triggered by polyploidy and/or hybridization. The objectives of this work were to characterize and compare the reproductive development and the timing of apospory initial (AI) emergence between diploid genotypes with potential for apomixis and facultative apomictic tetraploid cytotypes of *P. rufum*.
• **Methods** Reproductive characterization was performed by cytoembryological observations of cleared ovaries and anthers during all reproductive development steps and by quantitative evaluation of the ovule growth parameters.
• **Key Results** Cytoembryological observations showed that in diploids, both female and male reproductive development is equally synchronized, but in tetraploids, megasporogenesis and early megagametogenesis are delayed with respect to microsporogenesis and early microgametogenesis. This delay was also seen when ovary growth was taken as a reference parameter. The analysis of the onset of AIs revealed that they emerge during different developmental periods depending on the ploidy level. In diploids, the AIs appeared along with the tetrad (or triad) of female meiocytes, but in tetraploids they appeared earlier, at the time of the megaspore mother cell. In both cytotypes, AIs can be seen even during megagametogenesis.
• **Conclusions** Overall observations reveal that female sexual reproductive development is delayed in tetraploids as compared with diploid genotypes, mainly at meiosis. In tetraploids, AIs appear at earlier sexual developmental stages than in diploids, and they accumulate up to the end of megasporogenesis. The longer extension of megasporogenesis in tetraploids could favour AI emergence and also apomixis success.

Keywords: Apomixis, apospory initial, apospory, heterochrony, *Paspalum rufum*, reproductive development, polyploidy, sexuality.

INTRODUCTION

Apomixis in angiosperms is an asexual mode of reproduction by seeds that generate maternal clonal progeny (Nogler, 1984). In gametophytic apomixis, embryo sacs carrying non-reduced nuclei are generated after a series of mitoses. According to the origin of the non-reduced megagametophytes, apomixis can be divided into: 'diplospory', where they develop from the megaspore mother cell (MMC) itself, after failing or skipping meiosis, and 'apospory', where they arise from somatic nucellar cells (apospory initials, AIs) (Nogler, 1984; Savidan, 2000, 2001). Both processes include the fertilization-independent embryo development from an unreduced egg cell (parthenogenesis) and the autonomous endosperm formation or after central cell fertilization by one sperm nucleus (pseudogamy) (Nogler, 1984; Asker and Jerling, 1992).

Gametophytic apomixis in grasses is strongly linked to polyploidy, and usually apomictic species form multiploid complexes including sexual self-sterile diploid and apomictic self-fertile polyploid cytotypes (Savidan, 2000). Nevertheless, some species of the genus *Paspalum* and *Brachiaria* present diploid individuals with the capacity to form unreduced embryo sacs and occasionally to complete the whole apomixis process (Quarin, 1986; Quarin and Norrmann, 1987; Norrmann *et al.*, 1989; Naumova *et al.*, 1999; Quarin *et al.*, 2001; Siena *et al.*, 2008; Delgado *et al.*, 2014). In dicotyledonous plants, diplosporous apomixis is widely found at the diploid level in the *Boechera* complex (Schranz *et al.*, 2005; Aliyu *et al.*, 2010).

Most apomictic polyploids are facultative (i.e. apomixis and sexuality coexist in the same plant and even in the same ovule) expressing residual sexuality in different proportions (Nogler, 1984; Asker and Jerling, 1992; Ozias-Akins and van Dijk,

© The Author(s) 2018. Published by Oxford University Press on behalf of the Annals of Botany Company.
All rights reserved. For permissions, please e-mail: journals.permissions@oup.com.

2007). In these systems, sexual and apomictic reproductive pathways develop simultaneously and compete for seed formation (Hojsgaard *et al.*, 2013). Therefore, both sexuality and apomixis coexist in most apomictic species, and the prevalence of one type of reproduction over the other depends on one or several still unknown factors.

Apomixis is considered to have evolved in plants as an alternative reproductive system through the rearrangement of developmental programmes that constitute the normal sexual pathway (Grimanelli *et al.*, 2001). Evidence in *Hieracium* supports this idea, where apomixis and sexuality are superimposed and inter-related processes (Tucker *et al.*, 2003; Koltunow *et al.*, 2011). While the sexual pathway seems to stimulate AI formation, the apomictic pathway may function to recruit the sexual machinery at a specific time to enable apomixis. This observation suggests that apomixis is not a completely independent pathway but, if the apomictic pathway is not initiated, the sexual pathway remains functional (Koltunow *et al.*, 2011; Hand and Koltunow, 2014). Moreover, mutants of sexual species showing phenotypes reminiscent of apomictic components, such as the production of unreduced gametes and the formation of multiple embryo sacs, were described (Garcia-Aguilar *et al.*, 2010). Mutants of *Argonaute 9*, a gene related to silencing of transposable elements (TEs) in female gametes, and of *RDR6* and *SGS3*, related to small interfering RNA (siRNA) biogenesis, lead to the differentiation of multiple gametic cells that can initiate gametogenesis (Olmedo-Monfil *et al.*, 2010; Hernández-Lagana *et al.*, 2016). Similar phenotypes were also observed in mutants of the members of the RNA-directed DNA methylation (RdDM) pathway (*DMT102*/*DMT105*/*CMT3*, *DMT103*/*DRM1* and *CHR106*/*DDM1*) (Garcia-Aguilar *et al.*, 2010). In *Arabidopsis thaliana*, clonal seeds were obtained by combining the mutants *dyad* and *MiMe* with *GEM* lines (Marimuthu *et al.*, 2011). Moreover, *in vitro* culture conditions and/or the addition of exogenous steroid hormones induce autonomous endosperm development in arabidopsis ovules (Rojek *et al.*, 2015). All the above information reveals that a deregulation of the sexual controlling mechanism can generate phenotypes that mimic apomixis components. Also, in several *Paspalum* spp., the duplication of the chromosome content by colchicine treatment of sexual diploids generates tetraploid apomictic plants (Quarin and Hanna, 1980; Quarin *et al.*, 1998, 2001).

Carman (1997) postulated the 'duplicate-gene asynchrony hypothesis' proposing that after (allo)polyploidization, the duplicate genes involved in female development are asynchronously expressed, which induces apomixis, polyspory and polyembryony by ectopically or prematurely expressing their developmental programmes (Carman, 1997). Hence, it would be interesting to analyse the synchronization and timing of aposporous initials at different ploidy levels in individuals with the capacity for both sexuality and apomixis.

Traditionally, the timing of reproductive development was assessed by determining ovule growth parameters, and the term 'heterochrony' was applied to denote differences between individuals in the timing of the onset or rate of development of a given cell or cell lineage relative to other cells or cell lineages (Bradley *et al.*, 2007). Acording to Carman's theory, some aposporous species of the genera *Paspalum*, *Poa*, *Ranunculus* and *Hieracium* have shown that the different events in apomictic development show high variability, which contrasts with sexual processes that are more strictly controlled (Koltunow *et al.*, 1998). In *Hieracium*, the apomictic events are stochastic, as the developmental events are somewhat randomly determined, differing from sexuality in which the timing of the reproductive developmental process is precisely co-ordinated (Koltunow *et al.*, 1998). Differential synchronization between developmental events was reported for aposporous *Hypericum*, where later megagametophyte developmental stages are delayed with respect to sexual accessions (Galla *et al.*, 2011). Also, in *Brachiaria decumbens*, sexual diploid and apomictic tetraploid development showed some differential synchronization, i.e. meiocytes are present up to later ovule developmental stages in apomictic genotypes (Dusi *et al.*, 1999). In *Sorghum bicolor* – an ancient diploidized paleotetraploid that can produce aposporous embryo sacs (AESs) – the characterization of female reproductive development of different apomictic genotypes found that the apospory programne heterochronically accelerates the onset of meiosis and sexual embryo sac formation (Carman *et al.*, 2011). Moreover, heterochrony in reproductive development was detected among sexual diploids (Bradley *et al.*, 2007) and also among sexual and apomictic genotypes of *Tripsacum* diplosporous species (Leblanc *et al.*, 1995; Grimanelli *et al.*, 2003). Leblanc *et al.* (1995) have shown that the first mitosis in diplosporic megagametophytes occurs at almost the same time – judging from the integument growth – as meiosis in sexual megasporocytes. On the other hand, Grimanelli *et al.* (2003) found that *Tripsacum* diplosporous ovules at the same developmental stage present meiocytes at different developmental stages in contrast to the exact co-ordination between ovule and reproductive development found in sexual genotypes. Heterochrony has also been evidenced as precocious (before anthesis) embryo development among diplosporous and aposporous apomictic species such as *Poa pratensis* (Yudakova and Shakina, 2007), *Paspalum* spp. (Burson and Bennett, 1970, 1971; Quarin and Burson, 1991; Quarin *et al.*, 1996), *Tripsacum* (Grimanelli *et al.*, 2003) and *Cenchrus ciliaris* (Sharma *et al.*, 2014).

Paspalum rufum Nees ex Steud. is a perennial grass native to Paraguay, southern Brazil, Uruguay and north-eastern Argentina (Quarin *et al.*, 1998). The species forms a multiploid complex including sexual self-sterile diploids and tetraploid apomictic self-fertile genotypes (Norrmann *et al.*, 1989). Natural diploid populations have previously been classified as sexual because under open pollination they complete the seed set only sexually (Norrmann *et al.*, 1989; Sartor *et al.*, 2011). However, some individuals present a relatively high proportion of AESs and are able to complete apomixis in low proportions under induced self-pollination or in interploidy crosses (Siena *et al.*, 2008; Sartor *et al.*, 2011; Delgado *et al.*, 2014). Tetraploid races reproduced mainly by aposporous apomixis (Sartor *et al.*, 2011). Thus, both diploid and tetraploid cytotypes are able to produce seeds by sexuality and apomixis. Nevertheless, sexuality prevails in diploids and apomixis in tetraploids. It is likely that if apomixis potential is present at both ploidy levels, the success of one reproductive mode over the other might rely on differential synchronization of the reproductive developments occurring at the different ploidies. To assess this hypothesis,

we compared the synchronization of sexual reproductive developmental processes by building reproductive calendars and determining the timing of AI emergence in both diploid and tetraploid genotypes of *P. rufum.*

MATERIALS AND METHODS

Plant material

Three diploid ($2n = 2x = 20$) and three tetraploid ($2n = 4x = 40$) genotypes of *P. rufum* were used. R5#49 is a diploid natural accession that showed about 13 % of their ovules bearing AESs and can complete apomixis (Delgado *et al.*, 2014) (Table 1). Diploid genotypes H#31 and H#39 are hybrid individuals, belonging to a previously developed F_1 segregating population (R6#45 × R5#49) that produced a relatively high proportion (between 22 and 35 %) of ovules containing an AES (Delgado *et al.*, 2016) (Table 1; Supplementary Data Table S1). Moreover, three tetraploid facultative apomictic accessions were used: Q3756 (Norrmann *et al.*, 1989), Q4185 (Quarin *et al.*, 1998), which showed a very high proportion of AESs (96.2 and 81.4), and Q3785 which was classified as apomictic by flow cytometry seed set analysis (FCSS) by Galdeano *et al.* (2016) (Table 1). Plants were grown and maintained under natural conditions in the field.

Cytoembryological observations

Inflorescences at different developmental stages were fixed in FAA (70 % ethanol, glacial acetic acid, formaldehyde, in the proportion 90:5:5) and transferred to 70 % ethanol for at least 24 h. Dissected pistils were clarified following the protocol described by Young *et al.* (1979). Ovules were observed with a light transmission Leica DM2500 microscope equipped with a differential interference contrast (DIC) system and a digital camera (Leica Microsystems DFC 295, Wetzlar, Germany). The ovary sections were also observed using safranin-fast green staining following the protocol described by Siena *et al.* (2008). The observations were carried out with a light transmission microscope (Nikon E200). The embryo sac types were classified according to the method of Norrmann *et al.* (1989). Briefly, embryo sacs showing the egg apparatus, two polar nuclei and a group of antipodal cells were classified as meiotic of the *Polygonum* type. Embryo sacs showing the egg apparatus and two polar nuclei, but lacking antipodal cells, were regarded as AESs of the *Paspalum* type (Siena *et al.*, 2008). Pollen development was evaluated by light microscopy, staining anthers at different developmental stages with a drop of 2 % (w/v) acetocarmine in accordance with the method of Laspina *et al.* (2008).

Analysis of reproductive development

Female reproductive development was divided into six developmental stages as specified in Fig. 1A. Stage I when an MMC is clearly visible within the ovule; stage II when both the dyad and tetrad from the MMC meiosis are present; and stage III, when the functional megaspore (FM) is present and the degenerated products of meiosis are still visible. Subsequent stages (IV, V and VI) include female gametophyte (FG) development during three rounds of mitosis and cellularization in accordance with previous arabidopsis classification (Christensen *et al.*, 1997): stage IV is a two nucleate FG after the first mitosis (FG2); stage V groups together the later megagametogenesis developmental stages after the second mitosis (FG4) and the third mitosis (FG5) up to cellularization of the embryo sac (FG4–FG6); and stage VI corresponds to a completely developed embryo sac at anthesis. On the other hand, male reproductive development was divided into five developmental stages. Stage I, when the microspore mother cells (MiMCs) are present in the anther; stage II, during meiosis including both the dyad and tetrad; stage III, when the unicellular microspore without any vacuole is visible; stage IV, when the vacuolated unicellular microspore is distinguished; and stage V, when the bicellular pollen grain is present (Fig. 1A).

TABLE 1. *Description of the* P. rufum *genotypes analysed*

Genotype	Ploidy level	Cytoembryological characterization		Mode of reproduction after*		Origin	Reference
		%AES†	%MES‡	Open pollination	Interspecific interploidy cross (%)§		
R5#49	2*x*	13	70.7	Sexuality	Sexuality/apomixis (15)	Corrientes, Argentina Saladas	Delgado *et al.* (2014)
H#31	2*x*	22.2	94.4	ND	Sexuality/apomixis (2)¶	Hybrid from R5#49 × R6#45	Delgado *et al.* (2016)
H#39	2×	35.85	82.9	ND	Sexuality/apomixis (0.8)¶	Hybrid from R5#49 × R6#45	Delgado *et al.* (2016)
Q3756	4*x*	96.2	ND	ND	ND	Uruguay: unknown locality, germplasm BR 2186	Norrmann *et al.* (1989)
Q4185	4*x*	81.4	11.6	ND	ND	BIII hybrid from 3754 (2*x*) × 3756 (4*x*)	Quarin *et al.* (1998)
Q3785	4*x*	52.7	58.6	Apomixis	ND	Corrientes, Argentimna 39 km North of Paso de los Libres	Espinoza (2002); Galedeano *et al.* (2016)

*Mode of reproduction determined by the flow cytometric seed screen method (FCSS) as described by Matzk *et al.* (2000).

†Proportion of ovules containing aposporous embryo sacs or aposporous and meiotic embryo sacs at anthesis.

‡Proportion of ovules containing a meiotic embryo sac at anthesis.

§Percentage of seeds produced by apomixis.

¶For details, see Supplementary Data Table S1.

ND, not determined.

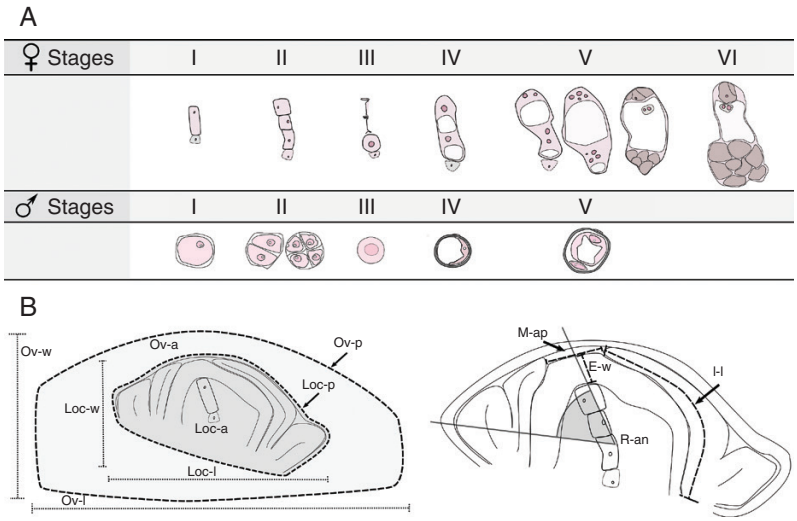

FIG. 1. Scheme of female and male reproductive developmental stages and quantitative ovule developmental parameters analysed. (A) The upper panel describes the six female developmental stages considered: megaspore mother cell (I), tetrad or triad just after meiosis has occurred (II), functional and degenerated megaspores (III) and the two nucleate megagametophyte just after the first mitosis (IV; FG2). Subsequent stages include four and eight nucleate megagametophytes after the second and third mitosis, and megagametophyte cellularization (V; FG4–FG6) and finally the mature megagametophyte at anthesis (VI) (from stages I to IV, LSCs are shown with dashed lines and micropylar and chalazal ends are in the top and in the lower sides, respectively). Nucleoli are shown in dark pink, vacuoles in white and megagametophyte cells in brown. In the lower panel, the five male reproductive developmental stages considered are specified: microspore mother cell (I), dyad and tetrads (II), unicellular microspore (III), vacuolated unicellular microspore (IV) and bicellular pollen grain (V). Nucleoli and vacuoles are shown in white and the nucleus is in dark pink. (B) Diagram describing ovary growth variables: locule width, Loc-w; locule length, Loc-l; locule perimeter, Loc-p; locule area, Loc-a (dark grey); ovary width, Ov-w; ovary length, Ov-l; ovary perimeter, Ov-p; ovary area, Ov-a (light grey); integument length, I-l; epidermis width, E-w; micropyle aperture, M-ap; and rotation angle, R-an.

In order to describe the reproductive development based on quantitative parameters, the following ovary developmental variables were considered. Ovary and locule (which coincides with ovule): width (Ov-w, Loc-w); length (Ov-l, Loc-l, µm); perimeter (Ov-p, Loc-p, µm) and area (Ov-a, Loc-a, μm^2); integument length (I-l, µm), micropyle aperture (M-ap, µm) and epidermis width (E-w, µm). Also, the ovule rotation angle (R-an, °) was determined by inscribing a line from the micropyle aperture midpoint to the ovule base and another line along the ovule's longitudinal axis (between the most distant points of the outer integuments). The inscribed angle was measured. The maximal angle is at the earliest developmental stage, and it reduces as development continues (Fig. 1B). The measurements were obtained from optical images of sagittally oriented ovaries by Image J analysis software (Schneider *et al.*, 2012). Ovary measurements were taken from a total of 469 ovaries, 265 and 204 for diploid and tetraploid cytotypes, respectively, and 8–86 ovaries per stage per cytotype (Supplementary Data Table S2). All the parameters were standardized to make them size independent, except for the ovule R-an. Quantitative parameters related to ovary, locule and epidermis were standardized by dividing each independent value by their mean value at anthesis. I-l was standardized by dividing it by the Loc-p value at each developmental stage, and M-ap was standardized by the Loc-l value at each developmental stage.

For quantitative comparison of the female and male development within each cytotype, spikelets at the same male reproductive development stage, as determined by acetocarmine staining of the anther, were collected. Pistils were dissected from the classified spikelets and cleared as described above. In some cases, pistils with their anther attached were cleared to observe both male and female development.

Statistical analysis

Comparisons between diploid and tetraploid ovary growth parameters were performed using the *t*-test or the Wilcoxon single rank test at a threshold value of $P < 0.01$. A multiple variance test and Kruskall–Wallis test were used to compare the growth parameters during the development in each cytotype by using STATGRAPHIC Plus 5.0 (Statgraphics.Net, Madrid, Spain) and InfoStat 2011e (Di Rienzo *et al.*, 2011). All size-independent parameters were used to obtain a Euclidean distance matrix between all developmental stages. An agglomerative hierarchical clustering algorithm based on Euclidean distance measures was used to cluster the developmental stages of both cytotypes. The unweighted pair group method with arithmetic mean (UPGMA) clustering algorithm was performed using InfoStat 2011e (Di Rienzo *et al.*, 2011). The cophenetic correlation coefficient was determined to test the goodness of the fit of the generated dendrogram.

RESULTS

Sexual reproductive development in diploid and tetraploid cytotypes

The characterization of the reproductive developmental stages of *P. rufum* was carried out by cytoembryological observations of cleared or stained ovules from differentiation of the MMC and MiMC, up to the mature embryo sac and pollen at the time of anthesis. Moreover, the spatial and temporal distribution of female megasporogenesis and megagametogenesis as well as male microsporogenesis and microgametogenesis were determined.

Analysis showed that female sexual reproductive development was very similar in both diploid and tetraploid cytotypes. The initial stage began with the differentiation of the archesporial cell from the nucellus to generate an easily recognizable MMC, which consisted of an enlarged cell of rectangular shape (Fig. 2A, D). The MMCs appeared under the ovule epidermis (layer 1-L1), which in diploids is of one cell width (Fig. 2A) and in tetraploids is of two or three cells (Fig. 2D). At the chalazal end of the MMC, a large cell, called the large stack cell (LSC), was frequently observed as previously described in *Sorghum* by Carman *et al.* (2011) (Fig. 2A, B, D). They were similar to meiocytes and remained visible throughout development up to stage III (not shown). In both cytotypes, meiosis yielded linear tetrads (Fig. 2B) but, frequently, linear triads were also evident (Fig. 2E). After completing meiosis, micropylar meiocytes degenerated and the FM differentiated in the centre of the ovule. At the end of megasporogenesis, an enlarged FM and degenerate meiocytes were observed (Fig. 2C, F). The diploid ovaries at stage II, and the tetraploid ovaries at stage I (MMC), showed periclinal divisions of the epidermis, giving rise to pseudocrassinucellate ovules (Fig. 2B, D).

Regarding ovary development, it was observed that the outer integument was fairly short throughout development and only the inner integument grew to define the micropyle, generating an endostomic ovule. The inner integument grows during meiosis leaving a micropylar aperture of about 3–4 cell widths (Fig. 2E). It then continues to grow along with the embryo sac cellularization, reaching its final length at anthesis (Fig. 2A–N).

Mitotic division of the FM gave rise to a meiotic embryo sac (MES) of the *Polygonum* type. Briefly at stage FG2, after the first mitosis, two polarized nuclei, separated by a large central vacuole, were produced, (Fig. 2G, J). Then, two additional mitotic divisions (Fig. 2H, I, K, L) gave rise to a mature embryo sac (Fig. 2M, N). At anthesis, the MES was characterized by the egg apparatus (one egg and two synergids), a large binucleate central cell with two polar nuclei and a mass of antipodal cells (Fig. 2M, N). Although female reproductive development showed the same main features in both cytotypes, differences in ovary development were visible. In the MMC, diploid ovaries seemed to be less developed than tetraploid ovaries, i.e. the locule was smaller, the ovule epidermis narrower and the inner integument shorter. Moreover, the ovule rotation was less advanced in diploids than in tetraploids (Fig. 2A, D). Similar differences were observed throughout reproductive development (Fig. 2).

Male reproductive development was initially characterized by the presence of MiMCs, stage I, located next to the tapetum cells. The MiMCs were easily identified by their large size, evident nucleoli and amorphous shape (Fig. 3A). Microsporogenesis proceeded with the first meiotic division, which resulted in a dyad (Fig. 3B), and then the second meiotic division occurred which resulted in isobilateral tetrads by successive cytokinesis, stage II (Fig. 3C). Afterwards a unicellular microspore containing a dense cytoplasm and a central nucleus was formed, stage III (Fig. 3D). Microgametogenesis started with the enlargement of a central vacuole and the concomitant displacement of the nucleus against the microspore wall; stage IV (Fig. 3E). Subsequently, the nucleus underwent the first pollen mitosis which resulted in the formation of a bicellular pollen grain containing two haploid nuclei, i.e. the vegetative nucleus and the generative nucleus; stage V (Fig. 3F).

Comparative analysis between female and male reproductive development showed that both processes were equally synchronized at the diploid level. Meiosis took place both in the anthers and in the ovules simultaneously (Supplementary Data Fig. S1A, B), and then a high degree of coincidence was observed in all developmental stages (Table 2). When anthers were at stage I and MiMCs were present, most of the ovules (95.8 %) also contained MMCs (Table 2; Supplementary Data Fig. S1A). Then as stage II proceeded and dyad/tetrads were present in anthers, 87.5 % of the ovules were also at stage II (Table 2) (Supplementary Data Fig. S1B). Likewise, while anthers were at stage III and unicellular microspores were just formed, 90.7 % of the ovules were mainly at stage III containing a FM. When the anther reached stage IV and contained a vacuolated unicellular microspore, 97.4 % of ovules also were at stage IV of megagametophyte development (Table 2).

In tetraploid genotypes, synchronization between male and female reproductive development showed some differences from diploid genotypes. Stage I was simultaneous in ovules and anthers; both MMCs and MiMCs were present in the same spikelet. However, when the anthers reached stage II and contained dyads or tetrads, MMCs were still present in the ovules (just 7.1 % of coincidence was detected at this stage) (Table 2; Supplementary Data Fig. S1C). Hereafter, when the anther reached stage III and microspores were formed, dyads/tetrads were present in most of the ovules and only 9.1 % of the ovules contained FMs (Table 2; Supplementary Data Fig. S1D). Finally, when microspores reached stage IV (vacuolated unicellular microspores), only 36 % of the ovules reached stage IV; the remainder were still at stage III (Table 2).

Quantitative characterization of ovule growth and development during female sexual reproductive development in diploid and tetraploid cytotypes

Ovary development was used as a reference parameter in assessing the timing of female reproductive development. Several ovary growth parameters were evaluated in both diploid and tetraploid cytotypes at different reproductive developmental stages (Supplementary Data Table S2). Then, the mean growth parameters were compared throughout development in both cytotypes (Fig. 4). At the diploid level, none of the parameters differed statistically between stages I and II (Fig. 4A). However, significant differences in several variables were detected from stages II to VI (Fig. 4A). All growth parameters were significantly different between stages II (dyad/tetrad) and III (FM). Between stages III and IV (FG2), six out of the 12 variables (Loc-l, Loc-p, Loc-a, Ov-a, I-l and R-an) increased significantly. Comparison between the subsequent stages (IV–VI) showed that almost all parameters increased significantly (Fig. 4A; Supplementary Data Table S2). These observations suggest that meiosis proceeded without any significant ovary growth. Then, during functional megaspore differentiation and megagametogenesis, the ovule size increases through all developmental stages up to anthesis. A similar analysis in tetraploids showed that all growth ovary parameters differed statistically

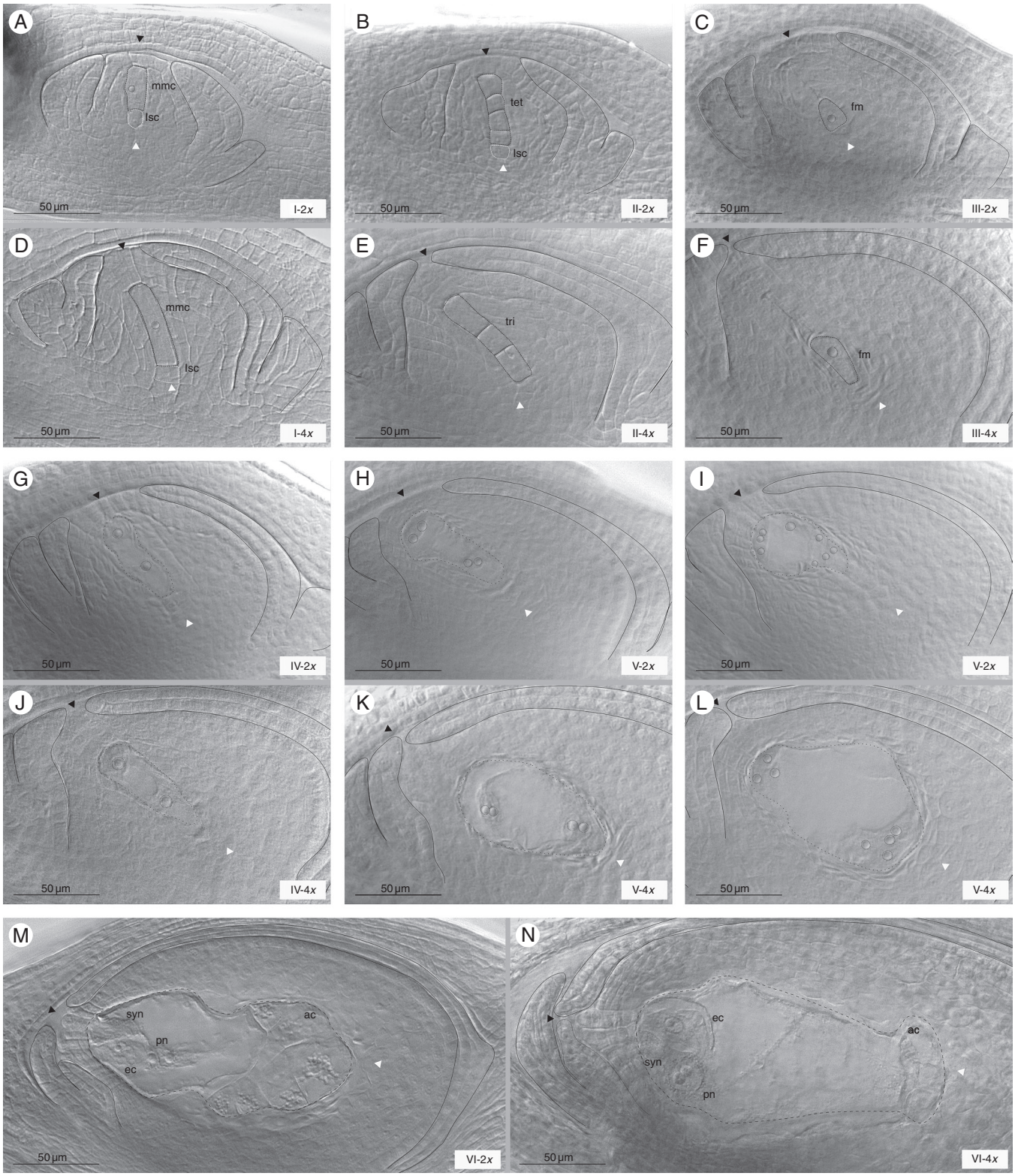

FIG. 2. Female sexual reproductive development in diploid and tetraploid cytotypes. Megasporogenesis in diploid (A–C) and tetraploid (D–F) cytotypes. (A and D) MMC (mmc); (B and E) tetrad/triad after meiosis (tet/tri); (C and F) functional megaspore (fm). Megagametogenesis in diploid (G–I) and tetraploid (J–L) cytotypes. (G and J) Two nucleate FGs after the first mitosis; (H and K) a four nucleate FG after the second mitosis and (I and L) an eight nucleate FG (outlined by short dashed black lines) after the third mitosis; (M and N) a mature female megagameophyte (outlined by large dashed black lines) containing one egg cell (ec), synergid cells (syn), a binucleate central cell (pn) and a group of antipodal cells (ac) at the anthesis developmental stage of diploid and tetraploid cytotypes, respectively. Structures and cells indicated are marked with black dashed lines, while the nucleolus is marked with black pointed lines. Large stack cells (lscs) are marked with white dashed lines. Micropylar and chalazal ends are indicated by black and white arrows respectively, and integuments are marked with black lines. Scale bars indicate 50 µm. Stages of development and ploidy levels are specified at the bottom right of each image. Genotypes shown in each image are: R5#49 (A, B), H#39 (C, G, H, I, M), Q3756 (D, N), Q3785 (E, L) and Q4485 (F, J, K).

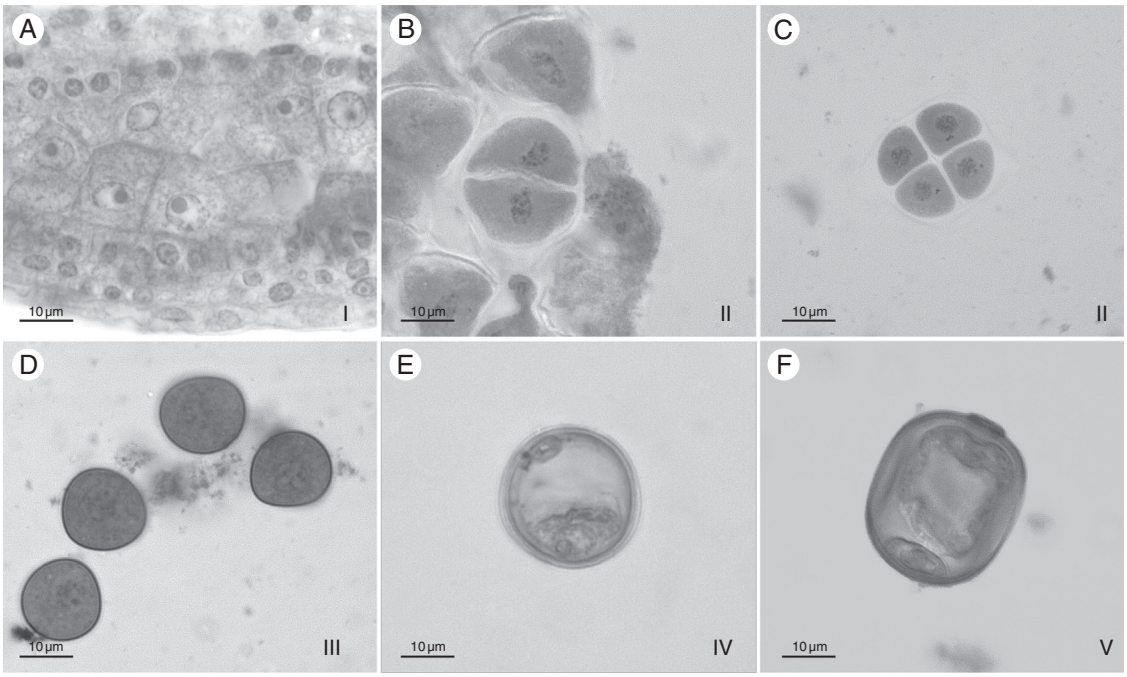

FIG. 3. Typical examples of the male sexual reproductive developmental stages observed. Anther showing (A) tapetum and MiMCs; (B) dyads just after the first meiotic division; (C) tetrads after the second meiotic division; (D) a recently formed unicellular microspore; (E) a vacuolated unicellular microspore; and (F) a bicellular pollen grain. Microspore and microgametophyte developmental stages are specified at the bottom right of each image. Scale bars indicate 10 µm. All images are of genotype H#39.

TABLE 2. *Levels of coincidence between female and male reproductive development in diploid and tetraploid genotypes of* P. rufum

		Male development*			
		MiMC (I)	Dyad/ tetrad (II)	Unicellular microspore (III)	Vacuolated unicellular microspore (IV)
Diploid					
Female development	I	**46**	4	1	0
	II	1	**30**	3	1
	III	1	1	**39**	0
	IV	0	0	0	**37**
	% coincidence†	95.8%	85.7%	90.7%	97.4%
Tetraploid					
Female development	I	**23**	**26**	2	0
	II	0	2	**8**	3
	III	0	0	1	**32**
	IV	0	0	0	20
	% coincidence†	100	7.1	9.1%	36%

Values in bold indicate the developmental stages with the highest number of ovaries scored.

*Number of spikelets at each female developmental stage found for a particular male developmental stage.

†Proportions of spikelets with the same male and female developmental stage.

between stages I and II (Fig. 4B), and almost all differesd between stages II, III and IV (Fig. 4B). From IV to V (FG4–FG6), there was not much growth variation and from V to VI, only Loc-l, Ov-p, E-w, M-ap and R-an showed significant differences (Fig. 4B; Supplementary Data Table S2). These outcomes indicate that in tetraploids the ovary growth and development occurred mainly between stage I and stage IV (Fig. 4B). Comparison of ovary development between cytotypes showed differences in the co-ordination of the ovary growth and female reproductive development.

In order to compare the co-ordination between female sexual reproductive development and ovary growth at both ploidy levels, the initial approach was to compare ovary parameters at each reproductive developmental stage between the two cytotypes (Supplementary Data Table S2 and Fig. S2). These analyses showed that all variables were higher for the six reproductive stages in tetraploid than in diploid cytotypes. In the case of M-ap, which decreased throughout development, it was always lower in tetraploids than in diploids (Supplementary Data Fig. S2; Table S2). These differences were observed at anthesis as well, indicating that tetraploid organs are larger than diploid organs.

In a second analysis, size-independent (SI) ovary parameters were evaluated. For this purpose, each ovary growth variable was standardized (as detailed in the Materials and Methods), except for R-an, which, *per se*, is size independent. Statistical analyses revealed that at earlier female reproductive developmental stages (from I to V), almost all SI variables presented higher mean values in tetraploid than in diploid cytotypes (Fig. 5A–C), (Supplementary Data Fig. S3; Table S3). However, at anthesis, non-significant differences for all variables between cytotypes were detected. Quantitative comparisons of SI ovary parameters showed that for the same female reproductive developmental stage, the tetraploid ovaries were more developed than those of the

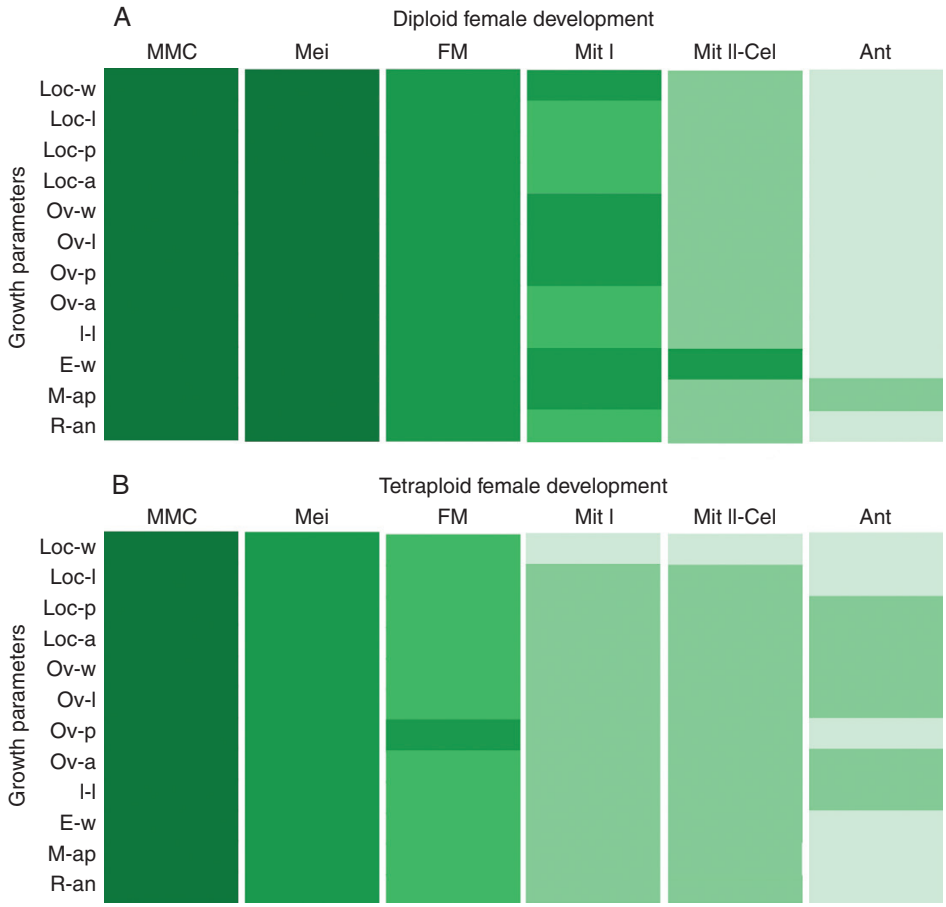

FIG. 4. Variation of ovary growth parameters throughout female sexual reproductive development in diploid and tetraploid cytotypes. Diagrams show 12 ovary growth parameters analysed during the six female developmental stages. Different cell colours indicate that the ovary growth parameters corresponding to different female sexual developmental stages are statistically significantly different ($P < 0.01$). Ovary parameters are specified: locule width, Loc-w; locule length, Loc-l; locule perimeter, Loc-p; locule area, Loc-a; ovary width, Ov-w; ovary length, Ov-l; ovary perimeter, Ov-p; ovary area, Ov-a; integument length, I-l; epidermis width, E-w; micropyle aperture, M-ap; and rotation angle, R-an. Female developmental stages are specified as described in the Materials and Methods.

diploids, which also agreed with the previous qualitative observations, indicating that diploid and tetraploid cytotypes present differential co-ordination between female reproductive development and ovary growth.

A cluster analysis that included all SI ovary growth parameters of both cytotypes was performed to find out which reproductive developmental stages of diploid and tetraploid cytotypes presented the same level of ovary growth. By this analysis, the female reproductive developmental stages that shared similar SI ovary growth parameters could be grouped together. The cophenetic correlation coefficient of the UPGMA dendrogram was 0.939 (Fig. 5D). The analysis showed four major clusters: one group contained ovaries at stage I of the two cytotypes and stage II of diploids; however, tetraploid ovaries containing an MMC presented a lower Euclidean distance with the diploid ovaries at stage II. The second cluster group contained tetraploid ovaries at stage II together with diploid ovaries at stage III and also at stage IV (FG2). The third cluster group contained tetraploid ovaries at megagametogenesis stages (III–V) and diploid ovaries at stages FG4–FG6 (V). Finally, the fourth cluster group contained ovaries of both cytotypes at anthesis (VI).

Aposporous initial observations in diploid and tetraploid cytotypes

To characterize the initial steps of the aposporous development at both ploidy levels, the differentiation of AIs in both cytotypes was determined. The AI cells were identified by their large size, tear shape and their dense and visible nucleoli (Fig. 6B–K). AIs in both diploid and tetraploid genotypes were detected at different stages of female sexual development starting before meiosis (in tetraploids) to FG5 of megagametogenesis (in diploids) (Fig. 6A). At more advanced developmental stages, AESs were more frequently observed than AIs. Proportions of ovaries containing AIs in all the female reproductive developmental stages are shown in Fig. 6A (and Supplementary Data Table S4). Interestingly, the AIs were always localized along with the MMC and/or meiocytes, indicating a strong relationship with the MMC differentiation signals (Fig. 6B, C). Frequently, LSCs, similar to AIs, were observed at the chalazal end, but no further development was detected in these cells (Fig. 6A, G, H).

In a few diploids, AIs first appeared along with tetrads at stage II (1.6 %; Fig. 6A, B) and could be observed up to FG5 in

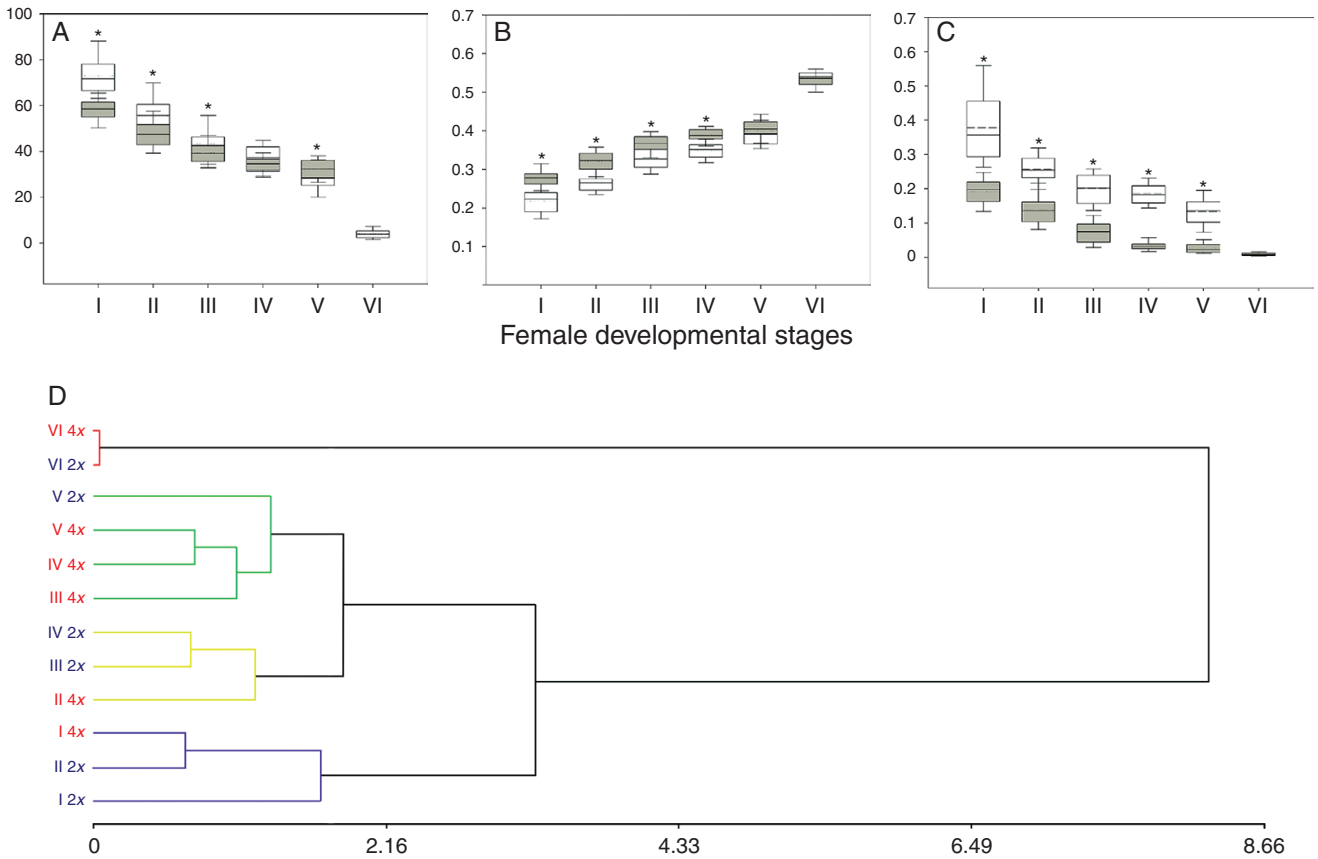

FIG. 5. Comparative analysis of ovule growth throughout female sexual development between diploid and tetraploid cytotypes. The first three panels (A–C) show box plot graphics of three size-independent (SI) ovary growth parameters of diploid (white) and tetraploid (grey) cytotypes: (A) rotation angle, (B) relative integument length and (C) relative micropyle aperture. Box limits represent the 25th and 75th percentiles; the full line inside the box designates the mean value, and dashed line the median value. Asterisks mark statistically significant differences between average values of SI ovule growth parameters. (D) Dendrograms derived from the UPGMA based on Euclidean distance include all the ovary SI parameters analysed at the six sexual female developmental stages scored in diploid and tetraploid cytotypes (cophenetic correlation coefficient: 0.939). The main clusters are shown in different colours (Euclidean distance cut-off, 1.75). Diploid and tetraploid cytotypes are expressed as 2*x* (blue) and 4*x* (red); sexual developmental stages are named as described before.

similar low proportions (1.6–4.3 %; Fig. 6A–F; Supplementary Data Table S4).

In tetraploids, the proportions of ovaries bearing AIs varied from about 8 % at MMC (Fig. 6A, G) to >21 % at the FM stage (Fig. 6A, I) (Supplementary Data Table S4). Furthermore, AIs were observed up to FG4, the second mitosis of megagametogenesis (Fig. 6A, J, K). The higher proportion of AIs was observed when FMs and degenerated megaspores were present (Fig. 6A, H, I), revealing a continuous AI differentiation during the female reproductive developmental stages (from I to III). The overall proportion of ovules bearing AIs was lower in diploids than in tetraploids, as expected. According to these results, regarding female sexual development, the onset of the AIs in tetraploids began earlier than in diploids. Cytoembryological analysis of diploid reproductive development revealed that mature AESs bear either one or two polar nuclei. The revision of previously obtained AES images (Delgado *et al.*, 2016), from 20 individuals of an F_1 population, showed that of the mature AESs analysed, 18 % had one polar nucleus and 82 % had two polar nuclei (Supplementary Data Table S5; Fig. S4).

As a general overview, Fig. 7 summarizes the information obtained in this work in order to build up a detailed reproductive calendar. Separate panels illustrate female sexual reproductive developmental stages for diploid and tetraploid *P. rufum* genotypes, and both are compared with male reproductive development. The period of AI detection was also described (blue bars).

DISCUSSION

Apomixis is widely distributed in angiosperms and is associated with polyploidy and hybridization. The trait is of great interest for plant breeding and food crop production since it can be used for stabilizing superior genotypes and fixing heterosis (Burton and Forbes, 1960; Vielle-Calzada *et al.*, 1996). However, major crops such as rice, maize, sorghum and wheat are not naturally apomictic, and attempts to introduce the trait from their wild relatives have been unsuccessful (Spielman *et al.*, 2003; Leblanc *et al.*, 2009). The manipulation of apomixis and its use in breeding programmes are still restricted to natural apomictic species, including several sub-tropical grasses (Miles, 2007; Acuña *et al.*, 2009, 2011; Jank *et al.*, 2011, 2014). However, most of these grasses are polyploid, highly heterozygous and genetically poorly characterized (Podio *et al.*, 2012*a*). The transference of apomixis to major diploid crops still requires the generation of fundamental knowledge about the molecular control and regulatory

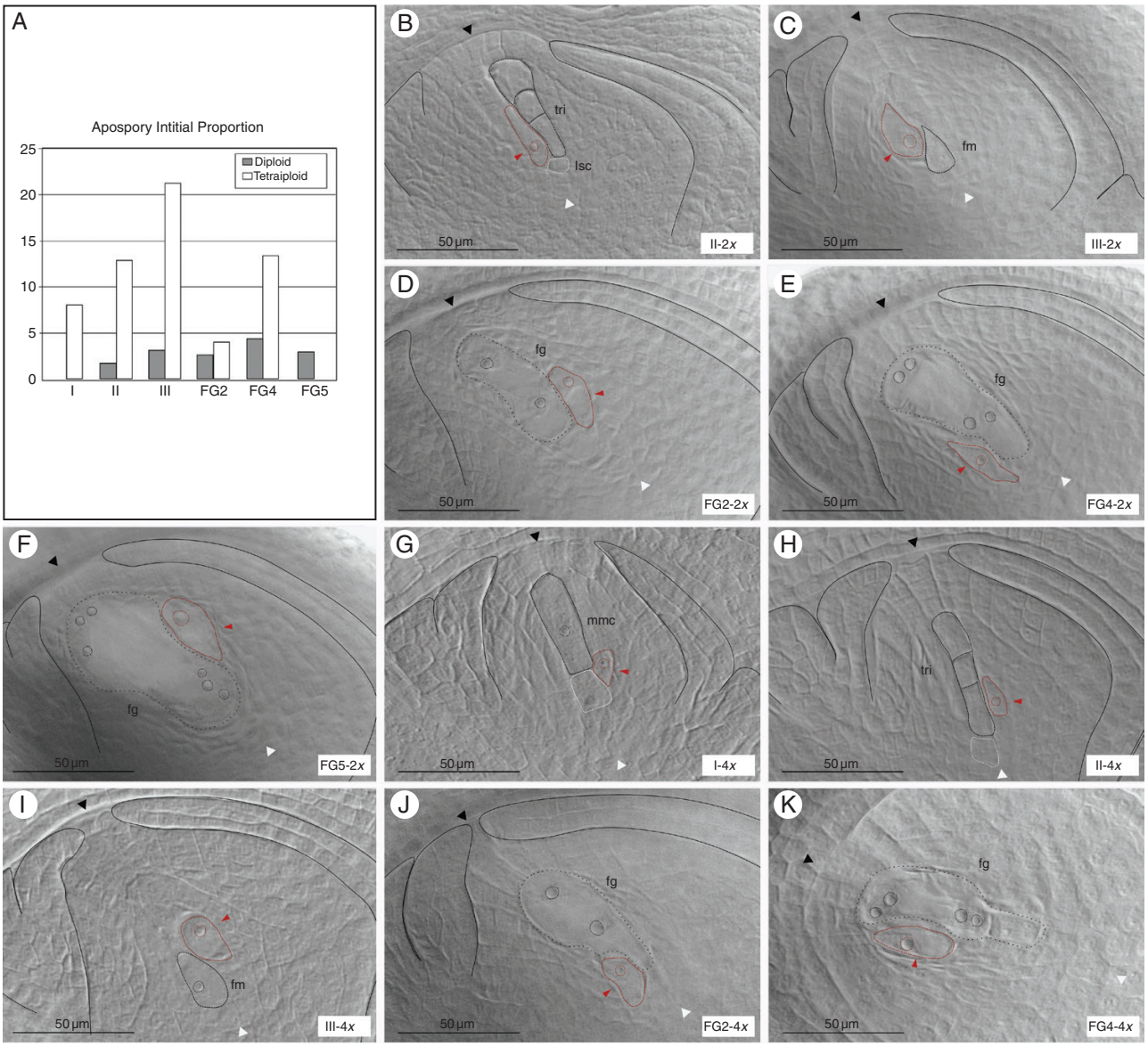

FIG. 6. AI emergence during sexual reproductive development in diploid and tetraploid cytotypes. (A) The proportion of ovaries containing AIs at each female reproductive developmental stage in diploid (grey) and tetraploid (white) cytotypes. (B–K) Cleared ovaries containing AIs at different female sexual developmental stages. In diploids: (B) triad (tri) after meiosis, (C) functional megaspore (fm); megagametogenesis stages after (D) the first mitosis, (E) the second mitosis and (F) the third mitosis (FG2, FG4 and FG5, respectively). In tetraploids: (G) MMC (mmc), (H) triad after meiosis, (I) functional megaspore, megagametogenesis stages after (J) the first mitosis and (K) the second mitosis. Red dashed lines and arrows indicate AIs. Structures and cells are marked with red/black dashed lines, while nucleoli are marked with black/red pointed lines. Large stack cells (lsc) are marked with white dashed lines. Micropylar and chalazal ends are indicated by black and white arrowheads, respectively, integuments are marked with black lines. Scale bars indicate 50 µm. Stages of development and ploidy levels are specified at the bottom right of each image. Genotypes of each image are: R5#49 (B), #31 (C), #39 (D–F), Q3756 (G–I), Q3785 (J) and Q4485 (K).

determinants of apomixis. The information acquired during the past years in *P. rufum* (Quarin and Norrmann, 1987; Quarin *et al.*, 2001; Siena *et al.*, 2008; Sartor *et al.*, 2011; Delgado *et al.*, 2014, 2016) has provided enough reasons to propose this multiploid complex as an interesting diploid/tetraploid system for studying the genetic and molecular determinants of aposporous apomixis at both diploid and polyploid levels. Molecular and functional analyses in this agamic complex will contribute to an understanding of the influence of polyploidy on the success of apomixis and the key element(s) that allow its expression in a diploid environment.

In this work, we present a detailed characterization of megasporogenesis and megagametogenesis, as well as microsporogenesis and microgametogenesis in diploid and tetraploid genotypes that can also reproduce by apomixis. Ovule growth and development were similar to previous descriptions in related species; pseudo-crassinucelated ovules were previously observed in other Panicoid species (Bhanwra *et al.*, 1988, 1991) and endostomic ovules were mainly observed in other grasses (Kellogg, 2015). Our results showed that *P. rufum* ovules rotated almost 90° during reproductive development, and so they are designated as hemianatropous (Sajo *et al.*, 2008). The

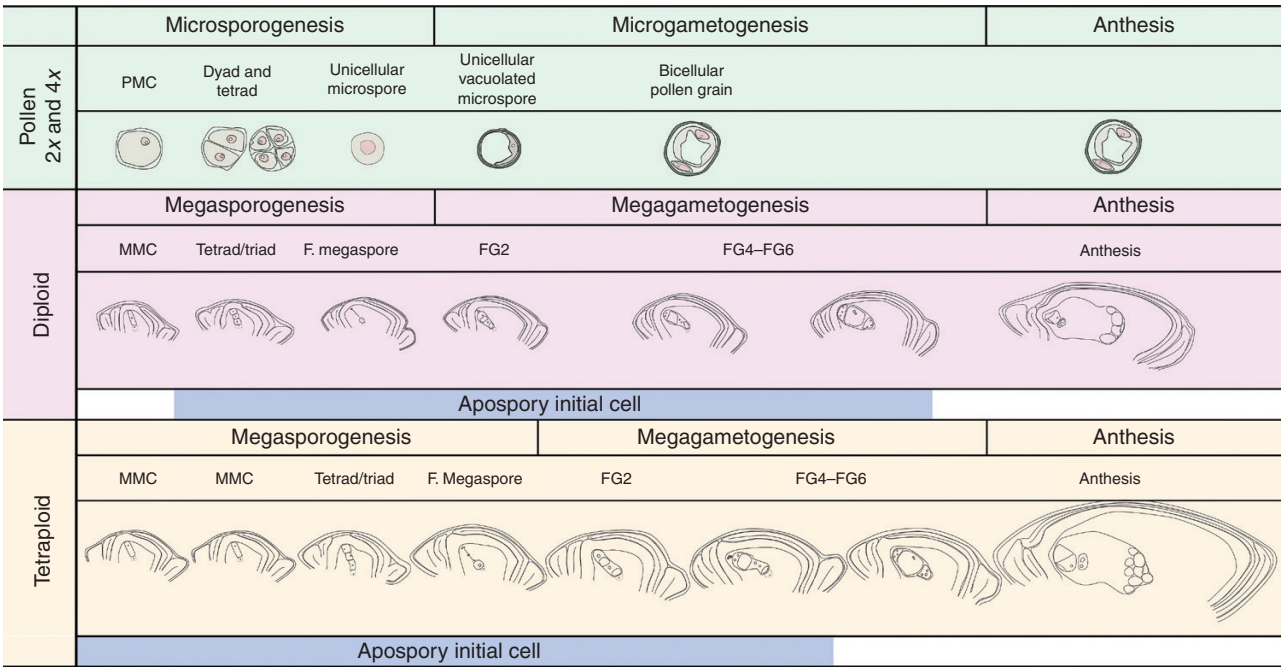

FIG. 7. Comparison of reproductive developmental processes in both diploid and tetraploid cytotypes. Diploid and tetraploid male reproductive development is described in the upper part of the panel (light green). Female sexual developmental stages for diploid (lilac) and tetraploid (light yellow) cytotypes are represented separately according to their synchronization with male reproductive development. The period during which AIs are present is also specified by a light blue coloured line at the bottom of each panel. LSCs are shown by dashed lines.

megaspore and megagametophyte development agreed with previous descriptions of the species of the subfamilies Pooideae and Panicoideae (Burson, 1985; Bhanwra *et al.*, 1991; Burson and Hussey, 1998). A typical feature frequently found was a linear triad, instead of a tetrad after meiosis. Other examples of triads were previously reported in other *Paspalum* species such as *Paspalum simplex* (Espinoza and Quarin, 1997), *P. malacophyllum*, *P. procurrens* (Hojsgaard *et al.*, 2008) and *Thrasya petrosal*, a grass closely related to *Paspalum* spp. (Acuña *et al.*, 2005), where the second meiotic division seems to take place only at the chalazal member of the dyad. On the other hand, during microsporogenesis, after MiMC differentiation, meiosis takes place, showing dyads and tetrads with successive division as in most grasses (Nakamura *et al.*, 2010; Kellogg, 2015). Microgametogenesis begins with formation of a central vacuole prior to the first mitosis, as was reported for maize and other grasses (Chang and Neuffer, 1989; Pacini *et al.*, 2011).

As was originally proposed by Carman (1997), there is strong evidence supporting heterochrony in reproductive developmental pathways between apomictic and sexual genotypes in several plant genera (Asker and Jerling, 1992; Leblanc *et al.*, 1995; Koltunow *et al.*, 1998; Grimanelli *et al.*, 2003; Bradley *et al.*, 2007; Carman *et al.*, 2011; Galla *et al.*, 2011; Sharma *et al.*, 2014). Therefore, *P. rufum* can be used for analysing the synchronization between reproductive developmental processes in genotypes with different ploidies and different apomixis capacities. Ovary growth parameters were used for comparing female sexual developmental processes. Interestingly, our results showed that diploid meiosis occurred without ovary growth, and at stages I and II the ovaries showed the same growth as tetraploid ovaries at stage I (MMC). On the other hand, in tetraploid genotypes, meiosis occurred along with significant ovary growth, that is similar to the growth observed for diploids at the FM stage and the first mitotic division of megagametophytes (IV). Moreover, tetraploid megagametophyte development (from IV to V) proceeded without any significant ovary growth, similar to diploid ovaries at stage V. These observations indicate delayed development of the tetraploid megaspore and early megagametophyte development with respect to diploid genotypes when judged from the growth of the ovaries.

Comparisons of both female and male reproductive development showed that in diploids, both male and female development from stages I to IV are perfectly co-ordinated. However, in tetraploids, female development was delayed with respect to microspore development and the early stage of microgametophyte development. This behaviour indicates that, in diploids, the signals for differentiation are simultaneously perceived in both processes. Similar behaviour was observed in *P. chaseanum*, *P. simplex* and *P. plicatulum* (Espinoza and Quarin, 1997). Such synchronization between male and female development in diploid sexual genotypes (where the male and female meiocytes arose simultaneously) was also detected in *Brachiaria decumbens* (Dusi and Willemse, 1999). On the other hand, in tetraploids, MiMC meiosis and the initial stage of microgametogenesis are advanced as compared with MMC meiosis and the initial stage of megagametogenesis. These results are consistent with previous cytoembryological studies of apomictic tetraploid *P. notatum* that have shown a similar asynchrony between male and female development (Bonilla and Quarin, 1997; Laspina *et al.*, 2008). Interestingly, in aposporous pentaploid *P. minus*, advanced microsporogenesis development was also observed with respect to megasporogenesis (Bonilla and Quarin, 1997), and similar results were reported for three facultative apomictic tetraploid species of *Brachiara* (Lutts *et al.*, 1994).

In previous works, the comparisons of reproductive development in apomictic species were referring to the ovary growth or male reproductive development, but the comparative systems used were different, making it difficult to arrive at a common understanding. Carman *et al.* (2011) for example, compared female sexual reproductive development between diploid genotypes of *Sorghum* that produce different proportion of AESs, and they found that apospory accelerates the onset of meiosis. However, the authors highlighted that none of the reports had provided convincing molecular or cytological evidence of parthenogenesis of the genotypes of these diploids. On the other hand, evidence of advanced or precocious aposporous or diplosporous development was reported for various genera (Asker and Jerling, 1992; Leblanc *et al.*, 1995; Peel *et al.*, 1997*a*, *b*; Koltunow *et al.*, 1998; Grimanelli *et al.*, 2003; Bradley *et al.*, 2007; Carman *et al.*, 2011; Galla *et al.*, 2011; Sharma *et al.*, 2014).

As was originally proposed by Carman (1997), allopolyploidy or hybrid origin could be the basis of asynchrony between developmental processes favouring apomixis expression. However, apomixis is not restricted to allopolyploidy. In the genus *Paspalum*, autopolyploidy or segmental allopolyploidy has usually been suggested as the origin of most apomictic tetraploids (Quarin, 1992; Quarin *et al.*,1998). Polyploid races of *P. rufum* probably derived from a natural autopolyploidization process through hybridization of non-reduced female gametes (Quarin *et al.*, 1998; Siena *et al.*, 2008). This system supports the hypothesis that autopolyploidy could also play an important role in the origin and evolution of apomixis in several warm-season grasses (Quarin *et al.*, 1998).

Moreover, autopolyploidy was also reported in other apomictic genera such as *Panicum* and *Tripsacum*, in which heterochrony was also detected (Grimanelli *et al.*, 1998, 2003; Bradley *et al.*, 2007). Therefore, heterochrony in the female developmental process occurring in tetraploid *P. rufum* could be a consequence of the effect of polyploidization *per se*. Strong evidence supports the fact that genome polyploidization would induce genomic re-arrangements, alteration of gene expression and genetic modifications at regions encoding retrotransposons, which would modulate transcription (Martelotto *et al.*, 2005, 2007; Podio *et al.*, 2012*b*; Ortiz *et al.*, 2013). Furthermore, the presence of TEs on the apomixis-controlling region (ACR) has been reported to be related to downregulation of gene expression (Ortiz *et al.*, 2013). In some *Paspalum* species, deregulation of gene expression was detected between apomictic and sexual genotypes (Laspina *et al.*, 2008; Polegri *et al.*, 2010; Ochogavia *et al.*, 2011).

Moreover, epigenetic differences were also well documented between apomictic and sexual *P. notatum* genotypes by Rodriguez *et al.* (2012), verifying the emergence of new epi-alleles after tetraploidization. A recent work published by Rodrigo *et al.* (2017) regarding the tetraploid apomictic weeping lovegrass reported an increment of expression of sexuality under stress conditions associated with epigenetic variation and TEs, supporting that apomixis vs. the sexual ratio would be subject to epigenetic control. By these antecedents, our results provide evidence of developmental heterochrony between reproductive processes associated with polyploidy, that could be related to the success of apomixis over sexuality at the tetraploid level.

Analysis of AIs revealed an extensive period of induction, starting before meiosis of the MMC up to the third mitotic division of megagametogenesis. At the diploid level, AIs were detected from stage II to stage FG5 in similar low proportions. However, in tetraploids, AIs were detected from stage I along with the MMC, up to stage FG4. Moreover, the highest proportion of AIs was detected at the FM stage. Therefore, it is possible that the female sexual reproductive developmental delay observed in tetraploids (in relation to ovule development and male reproductive development), and also detected in relation to emergence of the AI, would be associated with apomixis success. Related works on apomictic genotypes of *Paspalum* spp. show that AIs mainly appear along with the FM and sometimes with tetrads (Burson and Bennett, 1970, 1971; Quarin and Burson, 1991; Espinoza and Quarin, 1997; Quarin *et al.*, 1997, 2001). In the apomictic tetraploid of *B. briztha* and *B. decumbens*, AIs were reported to emerge along with the MMC (Dusi and Willemse, 1999; Lutts *et al.*, 1994). In aposporic diploid genotypes of *S. bicolor*, Carman *et al.* (2011) have reported detection of AIs along with the MMC, meiocyte, degenerating megaspores and the FM. Thus, it seems that the fate of nucellar cells could be modified along with different stages of the sexual pathway, mainly megasporogenesis, and their differentiation could rely on more than one specific molecular trigger.

These observations also align with previous works that reported a deregulation of genes related to sexual reproductive development between apomictic and sexual genotypes at early stages of development of sporogenesis. The *Somatic Embryogenesis Receptor Kinase* (*SERK*) gene, associated with the transition from somatic to embryogenic cells (Schmidt *et al.*, 1997), was found to be expressed in isolated cells of the nucellus of aposporous genotypes from *Paspalum* species but only in the MMC of sexual genotypes, suggesting a role in the specification of aposporous initials (Albertini *et al.*, 2005; Podio *et al.*, 2014). *Paspalum notatum Trimethylguanosine Synthase* (*TGS1*) that had been previously identified as downregulated during apomictic development (Pessino *et al.*, 2001; Laspina *et al.*, 2008) is expressed in the nucellus of sexual plants and its level increased with increases of sexuality of facultative apomictic genotypes from early developmental stages until maturity (Siena *et al.*, 2014). Analysis of arabidopsis mutants has also revealed that deregulation of genes related to female gamete formation, such as *Argonaute* 9 (*AGO9*), is associated with the formation of additional MMC-like cells in the ovule resembling apospory (García-Aguilar *et al.*, 2010; Olmedo-Monfil, 2010; Schmidt, 2015).

All the above information suggests that AIs are associated with early female reproductive developmental signals up to the FM stage. On the basis of our results, we propose that AIs accumulate during megaspore development, reaching their maximum at the FM stage, probably by a deregulated expression of genes related to megasporogenesis, suggesting that a longer extension of this period, like that observed in tetraploid genotypes, would imply a greater opportunity for AIs to emerge.

Additionally, it is important to highlight that from all the above analyses it could be deduced that AIs appear within the same ovary developmental period in both diploid and tetraploid genotypes irrespective of the heterochrony that is observed. Accordingly, ovary growth and developmental signals could

also be related to female reproductive development. It was recently reported that a gibberellin receptor gene, *Gibberellin-Insensitive Dwarf1* (*GID1*), is involved in both ovule growth/development and MMC differentiation. Its overexpression in arabidopsis induces both the presence of additional MMC-like cells and asynchrony in development of integument growth as regards megasporogenesis stages if compared with the wild type (Ferreira *et al.*, 2018). It is also well known that an ovular auxin gradient directs cell identity in the differentiated female gametophyte of arabidopsis, and acquisition of cell identity depends on the distance separating uncellularized haploid nuclei from the micropylar end of the ovule (Pagnussat *et al.*, 2009; Armenta-Medina *et al.*, 2011). Thereafter, both processes, i.e. ovule and female reproductive development, would be strongly inter-related and could also be related to AI differentiation.

Results presented in this work constitute the first exhaustive report on the chronology of sexual reproductive development and the presence of AIs in diploid and tetraploid genotypes of *Paspalum* spp. The detailed reproductive calendar of this multiploid complex allows us to determine the specific developmental stages to be selected in the future to identify key regulatory factors involved in the apomictic process.

SUPPLEMENTARY DATA

Supplementary data are available online at https://academic.oup.com/aob and consist of the following. Figure S1: cleared inflorescences showing both male and female reproductive development. Figure S2: quantitative comparison of ovary growth parameters between diploid and tetraploid cytotypes. Figure S3: quantitative comparison of ovary SI growth parameters between diploid and tetraploid cytotypes. Figure S4: diploid ovaries at anthesis showing MESs and AESs containing one and two polar nuclei. Table S1: reproductive mode of diploid hybrids H#31 and H#39. Table S2: statistical analysis of ovary growth parameters. Table S3: statistical analysis of ovary SI parameters. Table S4: detail of the proportions of ovaries bearing AIs at each developmental stage. Table S5: number of AESs bearing one or two polar nuclei in diploid *P. rufum* F_1 individuals.

ACKNOWLEDGEMENTS

We thank Drs Camilo Quarin and María Esperanza Sartor for providing some vegetal material. This work was supported by the Agencia Nacional de Promoción Científica y Tecnológica (ANPCyT), Argentina [PICT-2014-1080]; Consejo Nacional de Investigaciones Científicas y Técnicas (CONICET), Argentina, Projects [PIP 2012-2014 11420110100237 and PIP 2015–2017 11220150100702CO]; Universidad Nacional de Rosario (UNR), Argentina, Project [1AGR271 and AGR246]. M.S., F.E., J.P.A.O. and L.D. are research staff members of CONICET, Argentina.

LITERATURE CITED

Acuña CA, Martínez EJ, Quarin CL. 2005. Sexual diploid and apomictic tetraploid races in *Thrasya petrosa* (Gramineae). *Australian Journal of Botany* **53:** 479–484.

Acuña CA, Blount AR, Quesenberry KH, Kenworthy KE, Hanna WW. 2009. Bahiagrass tetraploid germplasm: reproductive and agronomic characterization of segregating progeny. *Crop Science* **49:** 581.

Acuña C, Blount AR, Quesenberry KH, Kenworthy KE, Hanna WW. 2011. Tetraploid bahiagrass hybrids: breeding technique, genetic variability and proportion of heterotic hybrids. *Euphytica* **179:** 227–235.

Albertini E, Marconi G, Reale L, *et al.* 2005. SERK and APOSTART. Candidate genes for apomixis in *Poa pratensis*. *Plant Physiology* **138:** 2185–2199.

Aliyu OM, Schranz ME, Sharbel TF. 2010. Quantitative variation for apomictic reproduction in the genus *Boechera* (Brassicaceae). *American Journal of Botany* **97:** 1719–1731.

Armenta-Medina A, Demesa-Arévalo E, Vielle-Calzada JP. 2011. Epigenetic control of cell specification during female gametogenesis. *Sexual Plant Reproduction* **24:** 137–147.

Asker SE, Jerling L. 1992. *Apomixis in plants*. Boca Raton, FL: CRC Press.

Bhanwra RK. 1988. Embryology in relation to systematics of Gramineae. *Annals of Botany* **62:** 215–233.

Bhanwra RK, Kaur N, Garg A. 1991. Embryological studies in some grasses and their taxonomic significance. *Botanical Journal of the Linnean Society* **107:** 405–419.

Bonilla JR, Quarin CL. 1997. Diplosporous and aposporous apomixis in a pentaploid race of *Paspalum* minus. *Plant Science* **127:** 97–104.

Bradley JE, Carman JG, Jamison MS, Naumova TN. 2007. Heterochronic features of the female germline among several sexual diploid *Tripsacum* L. (Andropogoneae, Poaceae). *Sexual Plant Reproduction* **20:** 9–17.

Burson BL. 1985. Cytology of *Paspalum chacoence* and *P. durifolium* and their relationship to *P. dilatatum*. *Botanical Gazette* **146:** 124–129.

Burson BL, Bennett HW. 1970. Cytology and reproduction of three *Paspalum* species. *Journal of Heredity* **61:** 129–132.

Burson BL, Bennett HW. 1971. Chromosome numbers, microsporogenesis, and mode of reproduction of seven *Paspalum* species. *Crop Science* **11:** 292–294.

Burson BL, Hussey MA. 1998. Cytology of *Paspalum malacophyllum* and its relationship to *P. juergensii* and *P. dilatatum*. *International Journal of Plant Sciences* **159:** 153–159.

Burton GW, Forbes I. 1960. The genetics and manipulation of obligate apomixis in common Bahia grass *Paspalum notatum* Flügge. In: *Proceedings of the Eighth International Grassland Congress*, held at the University of Reading, UK, 11–21 July 1960, 66–71.

Carman JG. 1997. Asynchronous expression of duplicate genes in angiosperms may cause apomixis, bispory, tetraspory, and polyembryony. *Biological Journal of the Linnean Society* **61:** 51–94.

Carman JG, Jamison M, Elliott E, Dwivedi KK, Naumova TN. 2011. Apospory appears to accelerate onset of meiosis and sexual embryo sac formation in sorghum ovules. *BMC Plant Biology* **11:** 9. doi: 10.1186/1471-2229-11-9.

Chang MT, Neuffer MG. 1989. Maize microsporogenesis. *Genome* **32:** 232–244.

Christensen CA, King EJ, Jordan JR, Drews GN. 1997. Megagametogenesis in Arabidopsis wild type and the Gf mutant. *Sexual Plant Reproduction* **10:** 49–64.

Delgado L, Galdeano F, Sartor ME, Quarin CL, Espinoza F, Ortiz JP. 2014. Analysis of variation for apomictic reproduction in diploid *Paspalum rufum*. *Annals of Botany* **113:** 1211–1218.

Delgado L, Sartor MaE, Espinoza F, Soliman M, Galdeano F, Ortiz JP. 2016. Hybridity and autopolyploidy increase the expressivity of apospory in diploid *Paspalum rufum*. *Plant Systematics and Evolution* **302:** 1471–1481.

Di Rienzo JA, Casanoves F, Balzarini MG, Gonzalez L, Tablada M, Robledo YC. 2011. *InfoStat version 2011*. Grupo InfoStat, FCA, Universidad Nacional de Córdoba, Argentina. http://www.infostat.com.

Dusi DMA, Willemse MTM. 1999. Apomixis in *Brachiaria decumbens* Stapf.: gametophytic development and reproductive calendar. *Acta Biologica Cracoviensia Series Botanica* **41:** 151–162.

Espinoza F. 2002. *Caracterización del comportamiento reproductivo en gramíneas subtropicales mediante marcadores moleculares y estudios embriológicos*. PhD Thesis, University of Rosario, Argentina.

Espinoza F, Quarin CL. 1997. Cytoembryology of *Paspalum chaseanum* and sexual diploid biotypes of two apomictic *Paspalum* species. *Australian Journal of Botany* **45:** 871–877.

Ferreira LG, de Alencar Dusi DM, Irsigler AST, *et al.* 2018. GID1 expression is associated with ovule development of sexual and apomictic plants. *Plant Cell Reports* **37:** 293–306.

Galdeano F, Urbani MH, Sartor ME, Honfi AI, Espinoza F, Quarin CL. 2016. Relative DNA content in diploid, polyploid, and multiploid species of *Paspalum* (Poaceae) with relation to reproductive mode and taxonomy. *Journal of Plant Research* **129:** 697–710.

Galla G, Barcaccia G, Schallau A, Molins MP, Bäumlein H, Sharbel TF. 2011. The cytohistological basis of apospory in *Hypericum perforatum* L. *Sexual Plant Reproduction* **24:** 47–61.

García-Aguilar M, Michaud C, Leblanc O, Grimanelli D. 2010. Inactivation of a DNA methylation pathway in maize reproductive organs results in apomixis-like phenotypes. *The Plant Cell* **22:** 3249–3267.

Grimanelli D, Leblanc O, Espinosa E, Perotti E, Gonzalez de LD, Savidan Y. 1998. Mapping diplosporous apomixis in tetraploid *Tripsacum*: one gene or several genes? *Heredity* **80:** 33–39.

Grimanelli D, Leblanc O, Perotti E, Grossniklaus U. 2001. Developmental genetics of gametophytic apomixis. *Trends in Genetics* **17:** 597–604.

Grimanelli D, Garcia M, Kaszas E, Perotti E, Leblanc O. 2003. Heterochronic expression of sexual reproductive programs during apomictic development in *Tripsacum*. *Genetics* **165:** 1521–1531.

Hand ML, Koltunow AM. 2014. The genetic control of apomixis: asexual seed formation. *Genetics* **197:** 441–450.

Hernández-Lagana E, Rodríguez-Leal D, Lúa J, Vielle-Calzada JP. 2016. A multigenic network of *ARGONAUTE4* clade members controls early megaspore formation in Arabidopsis. *Genetics* **204:** 1045–1056.

Hojsgaard D, Schegg E, Valls JFM, Martínez EJ, Quarin CL. 2008. Sexuality, apomixis, ploidy levels, and genomic relationships among four *Paspalum* species of the subgenus *Anachyris* (Poaceae). *Flora* **203:** 535–547.

Hojsgaard DH, Martínez EJ, Quarin CL. 2013. Competition between meiotic and apomictic pathways during ovule and seed development results in clonality. *New Phytologist* **197:** 336–347.

Jank L, Valle CB, Resende RMS. 2011. Breeding tropical forages. *Crop Breeding and Applied Biotechnology* **11:** 27–34.

Jank L, Barrios SC, do Valle CB, Simeão RM, Alves GF. 2014. The value of improved pastures to Brazilian beef production. *Crop and Pasture Science* **65:** 1132–1137.

Kellogg EA. 2015. *Flowering plants. Monocots*. Cham: Springer International Publishing.

Koltunow AM, Johnson SD, Bicknell RA. 1998. Sexual and apomictic development in *Hieracium*. *Sexual Plant Reproduction* **11:** 213–230.

Koltunow AM, Johnson SD, Okada T. 2011. Apomixis in hawkweed: Mendel's experimental nemesis. *Journal of Experimental Botany* **62:** 1699–1707.

Laspina NV, Vega T, Seijo JG, *et al.* 2008. Gene expression analysis at the onset of aposporous apomixis in *Paspalum notatum*. *Plant Molecular Biology* **67:** 615–628.

Leblanc O, Duenas M, Hernandez M, *et al.* 1995. Chromosome doubling in *Tripsacum*: the production of artificial, sexual tetraploid plants. *Plant Breeding* **114:** 226–230.

Leblanc O, Grimanelli D, Hernandez-Rodriguez M, Galindo PA, Soriano-Martinez AM, Perotti E. 2009. Seed development and inheritance studies in apomictic maize–*Tripsacum* hybrids reveal barriers for the transfer of apomixis into sexual crops. *International Journal of Developmental Biology* **53:** 585–596.

Lutts S, Ndikumana J, Louant BP. 1994. Male and female sporogenesis and gametogenesis in apomictic *Brachiaria brizantha*, *Brachiaria decumbens* and F 1 hybrids with sexual colchicine induced tetraploid *Brachiaria ruziziensis*. *Euphytica* **78:** 19–25.

Marimuthu MP, Jolivet S, Ravi M, *et al.* 2011. Synthetic clonal reproduction through seeds. *Science* **331:** 876.

Martelotto LG, Ortiz JPA, Stein J, Espinoza F, Quarin CL, Pessino SC. 2005. A comprehensive analysis of gene expression alterations in a newly synthesized *Paspalum notatum* autotetraploid. *Plant Science* **169:** 211–220.

Martelotto LG, Ortiz JP, Stein J, Espinoza F, Quarin CL, Pessino SC. 2007. Genome rearrangements derived from autopolyploidization in *Paspalum* spp. *Plant Science* **172:** 970–977.

Matzk F, Meister A, Schubert I. 2000. An efficient screen for reproductive pathways using mature seeds of monocots and dicots. *Plant Joural* **21:** 97–108.

Miles JW. 2007. Apomixis for cultivar development in tropical forage grasses. *Crop Science* **47** (Supplement 3): 238.

Nakamura AT, Longhi-Wagner HM, Scatena VL. 2010. Anther and pollen development in some species of *Poaceae* (Poales). *Brazilian Journal of Biology* **70:** 351–360

Naumova TN, Hayward MD, Wagenvoort M. 1999. Apomixis and sexuality in diploid and tetraploid accessions of *Brachiaria decumbens*. *Sexual Plant Reproduction* **12:** 43–52.

Nogler GA. 1984. Gametophytic apomixis. In: Johri BM, ed. *Embryology of angiosperms*. Berlin, Heidelberg: Springer, 475–518.

Norrmann GA, Quarin CL, Burson BL. 1989. Cytogenetics and reproductive behavior of different chromosome races in six *Paspalum* species. *Journal of Heredity* **80:** 24–28.

Ochogavía AC, Seijo JG, Gonzalez AM, *et al.* 2011. Characterization of retrotransposon sequences expressed in inflorescences of apomictic and sexual *Paspalum notatum* plants. *Sexual Plant Reproduction* **24:** 231–246.

Olmedo-Monfil V, Duran-Figueroa N, Arteaga-Vazquez M, *et al.* 2010. Control of female gamete formation by a small RNA pathway in Arabidopsis. *Nature* **464:** 628–632.

Ortiz JP, Quarin CL, Pessino SC, *et al.* 2013. Harnessing apomictic reproduction in grasses: what we have learned from *Paspalum*. *Annals of Botany* **112:** 767–787.

Ozias-Akins P, van Dijk PJ. 2007. Mendelian genetics of apomixis in plants. *Annual Review of Genetics* **41:** 509–537.

Pacini E, Jacquard C, Clément C. 2011. Pollen vacuoles and their significance. *Planta* **234:** 217–227.

Pagnussat GC, Alandete-Saez M, Bowman JL, Sundaresan V. 2009. Auxin-dependent patterning and gamete specification in the Arabidopsis female gametophyte. *Science* **324:** 1684–1689.

Peel MD, Carman JG, Leblanc O. 1997*a*. Megasporocyte callose in apomictic buffelgrass, Kentucky bluegrass, *Pennisetum squamulatum* Fresen, *Tripsacum* L., and weeping lovegrass. *Crop Science* **37:** 724–732

Peel MD, Carman JG, Liu ZW, Wang RRC. 1997*b*. Meiotic anomalies in hybrids between wheat and apomictic *Elymus rectisetus* (Nees in Lehm.) A. Löve & Connor. *Crop Science* **37:** 717–723

Pessino SC, Espinoza F, Martínez EJ, Ortiz JPA, Valle EM, Quarin CL. 2001. Isolation of cDNA clones differentially expressed in flowers of apomictic and sexual *Paspalum notatum*. *Hereditas* **134:** 35–42.

Podio M, Rodriguez MP, Felitti S, *et al.* 2012*a*. Sequence characterization, in silico mapping and cytosine methylation analysis of markers linked to apospory in *Paspalum notatum*. *Genetics and Molecular Biology* **35:** 827–837.

Podio M, Siena LA, Hojsgaard D, Stein J, Quarin CL, Ortiz JPA. 2012*b*. Evaluation of meiotic abnormalities and pollen viability in aposporous and sexual tetraploid *Paspalum notatum* (Poaceae). *Plant Systematics and Evolution* **298:** 1625–1633.

Podio M, Felitti SA, Siena LA, *et al.* 2014. Characterization and expression analysis of *SOMATIC EMBRYOGENESIS RECEPTOR KINASE* (*SERK*) genes in sexual and apomictic *Paspalum notatum*. *Plant Molecular Biology* **84:** 479–495.

Polegri L, Calderini O, Arcioni S, Pupilli F. 2010. Specific expression of apomixis-linked alleles revealed by comparative transcriptomic analysis of sexual and apomictic *Paspalum simplex* Morong flowers. *Journal of Experimental Botany* **61:** 1869–1883.

Rojek J, Pawełko Ł, Kapusta M, Naczk A, Bohdanowicz J. 2015. Exogenous steroid hormones stimulate full development of autonomous endosperm in *Arabidopsis thaliana*. *Acta Societatis Botanicorum Poloniae* **84:** 287.

Quarin CL. 1986. Seasonal changes in the incidence of apomixis of diploid, triploid, and tetraploid plants of *Paspalum cromyorrhizon*. *Euphytica* **35:** 515–522.

Quarin CL. 1992. The nature of apomixis and its origin in Panicoid grasses. *Apomixis Newsletter* **5:** 8–15.

Quarin CL, Hanna WW. 1980. Effect of three ploidy levels on meiosis and mode of reproduction in *Paspalum hexastachyum*. *Crop Science* **20:** 69–75.

Quarin CL, Norrmann GA. 1987. Cytology and reproductive behavior of *Paspalum equitans*, *P. ionanthum*, and their hybrids with diploid and tetraploid cytotypes of *P. cromyorrhizon*. *Botanical Gazette* **148:** 386–391.

Quarin CL, Burson BL. 1991. Cytology of sexual and apomictic *Paspalum* species. *Cytologia* **56:** 223–228.

Quarin CL, Pozzobon MT, Valls JFM. 1996. Cytology and reproductive behavior of diploid, tetraploid and hexaploid germplasm accessions of a wild forage grass: *Paspalum compressifolium*. *Euphytica* **90:** 345–349.

Quarin CL, Valls JFM, Urbani MH. 1997. Cytological and reproductive behaviour of *Paspalum atratum*, a promising forage grass for the tropics. *Tropical Grasslands* **31:** 114–116

Quarin CL, Norrmann GA, Espinoza F. 1998. Evidence for autoploidy in apomictic *Paspalum rufum*. *Hereditas* **129:** 119–124.

Quarin CL, Espinoza F, Martinez EJ, Pessino SC, Bovo OA. 2001. A rise of ploidy level induces the expression of apomixis in *Paspalum notatum*. *Sexual Plant Reproduction* **13:** 243–249.

Rodriguez MP, Cervigni GDL, Quarin CL, Ortiz JPA. 2012. Frequencies and variation in cytosine methylation patterns in diploid and tetraploid cytotypes of *Paspalum notatum*. *Biologia Plantarum* **56:** 276–282.

Rodrigo JM, Zappacosta DC, Selva JP, Garbus I, Albertini E, Echenique V. 2017. Apomixis frequency under stress conditions in weeping lovegrass (*Eragrostis curvula*). *PLoS One* **12:** e0175852. doi: 10.1371/journal.pone.0175852.

Sajo MG, Longhi-Wagner HM, Rudall PJ. 2008. Reproductive morphology of the early-divergent grass *Streptochaeta* and its bearing on the homologies of the grass spikelet. *Plant Systematics and Evolution* **275:** 245.

Sartor ME, Quarin CL, Urbani MH, Espinoza F. 2011. Ploidy levels and reproductive behaviour in natural populations of five *Paspalum* species. *Plant Systematics and Evolution* **293:** 31–41.

Savidan Y. 2000. Apomixis: genetics and breeding. *Plant Breeding Reviews* **18:** 13–86.

Savidan Y. 2001. Gametophytic apomixis. In: Bhojwani SS, Soh WY, eds. *Current trends in the embryology of angiosperms*. Dordrecht: Springer, 419–433.

Schmidt ED, Guzzo F, Toonen MA, de Vries SC. 1997. A leucine-rich repeat containing receptor-like kinase marks somatic plant cells competent to form embryos. *Development* **124:** 2049–2062.

Schmidt A, Schmid MW, Grossniklaus U. 2015. Plant germline formation: common concepts and developmental flexibility in sexual and asexual reproduction. *Development* **142:** 229–241.

Schneider CA, Rasband WS, Eliceiri KW. 2012. NIH Image to ImageJ: 25 years of image analysis. *Nature Methods* **9:** 671–675.

Schranz ME, Dobes C, Koch MA, Mitchell-Olds T. 2005. Sexual reproduction, hybridization, apomixis, and polyploidization in the genus *Boechera* (Brassicaceae). *American Journal of Botany* **92:** 1797–1810.

Sharma R, Geeta R, Bhat V. 2014. Asynchronous male/female gametophyte development in facultative apomictic plants of *Cenchrus ciliaris* (Poaceae). *South African Journal of Botany* **91:** 19–31.

Siena LA, Sartor ME, Espinoza F, Quarin CL, Ortiz JPA. 2008. Genetic and embryological evidences of apomixis at the diploid level in *Paspalum rufum* support recurrent auto-polyploidization in the species. *Sexual Plant Reproduction* **21:** 205–215.

Siena LA, Sartor ME, Quarin CL, Espinoza F, Ortiz JP. 2014. Transference of wheat expressed sequence tag simple sequence repeats to species and cross-species amplification of simple sequence repeats: potential use in phylogenetic analysis and mapping. *Crop Science* **54:** 240–254.

Spielman M, Vinkenoog R, Scott RJ. 2003. Genetic mechanisms of apomixis. *Philosophical Transactions of the Royal Society B: Biological Sciences* **358:** 1095–1103.

Tucker MR, Araujo AC, Paech NA, *et al.* 2003. Sexual and apomictic reproduction in *Hieracium* subgenus *pilosella* are closely interrelated developmental pathways. *The Plant Cell* **15:** 1524–1537.

Vielle-Calzada JP, Nuccio ML, Budiman MA, *et al.* 1996. Comparative gene expression in sexual and apomictic ovaries of *Pennisetum ciliare* (L.) Link. *Plant Molecular Biology* **32:** 1085–1092.

Young BA, Sherwood RT, Bashaw EC. 1979. Cleared-pistil and thick-sectioning techniques for detecting aposporous apomixis in grasses. *Canadian Journal of Botany* **57:** 1668–1672

Yudakova OI, Shakina TN. 2007. Specific features of early embryogenesis in apomictic *Poa pratensis* L. *Russian Journal of Developmental Biology* **38:** 1–6.